Dansylated Aminopropyl Controlled Pore Glass: A Model for Silica−Liquid Solvation[+]

Phillip M. Page, Chase A. Munson, and Frank V. Bright*

Department of Chemistry, Natural Sciences Complex, University at Buffalo, The State University of New York, Buffalo, New York 14260-3000

Received April 19, 2004. In Final Form: September 7, 2004

We have prepared a series of aminopropyl controlled pore glass (CPG) particles that have been labeled with a solvatochromic fluorescent probe molecule (dansyl). We report on the behavior of the attached dansyl reporter as a function of dansyl-to-amine molar ratio (i.e., dansyl loading), solvent dipolarity, and surface-residue end capping. In these experiments, we systematically adjust the dansyl loading by 10^5; a range much larger than ever explored. The dansylated CPG particles were also end capped with trimethylchlorosilane to derivatize most of the residual silanol and/or aminopropyl groups. The attached dansyl molecules can be surrounded by other dansyl molecules; they can be distributed within an ensemble of sites with differing physicochemical properties, and/or they can be distributed in sites that are restrictive to dansyl motion and/or solvent inaccessible. At high dansyl loadings, the majority of the dansyl groups are solvated by other dansyl moieties and solvent does not significantly alter the local microenvironment surrounding the average dansyl molecule (i.e., the cybotactic region) to any significant level. At intermediate dansyl loadings, the average distance between the dansyl groups increases and solvent is able to access/solvate/wet the dansyl groups and alter their cybotactic region to a greater extent. At the lowest dansyl loadings studied, the results suggest that these dansyl moieties are localized within solvent inaccessible/restrictive SiO_2 sites (e.g., small pores).

Introduction

The interaction of molecules covalently bonded to solid surfaces play important roles in many chemical processes and reactions (e.g., catalysis, chemical sensing, separations, and solid-phase synthesis). Thus, developing a more-detailed view of the solid−liquid interface is important to fully understand the role played by the surface. Specifically, information on the physical and physicochemical properties at the solid−liquid interface, including the nature of the attachment sites, the accessibility of the surface-bound species to solvent, (re)agents and analytes, and the local surface site dipolarity, are needed to provide a fundamental understanding of the local microenvironment surrounding surface-bound molecules attached to solid surfaces.

Controlled pore glass (CPG) is a commonly used solid support.[1−18] CPG-based materials are used as chromatographic stationary phases[1] and as an adsorption medium for a wide variety of reagents, such as biological macromolecules (e.g., proteins),[1−4] and various cations.[5−7] CPG is used as a solid support for immobilizing catalysts,[8,9] enzymes,[9,10] and nucleotides.[11] CPG has also been used in the solid-phase synthesis of macromolecules,[12,13] and it has served as a platform for immobilizing a wide variety of recognition elements for chemical sensing.[14−18]

CPG is a porous material with a surface that consists of siloxane and silanol groups.[1] Surface silanol groups provide attachment sites for the introduction of functional groups onto the CPG surface (e.g., amine groups) and are mostly responsible for the interactions between the CPG surface and potential adsorbates. The silanol groups are of three kinds: geminal, isolated, and vicinal or hydrogen-bonded.[19,20]

Aminopropyl-modified silica is a commonly used solid support that has been used for chemical separations,[21−24] surface catalysis,[25−28] chemical sensing,[29] and reagent

[+] Dedicated to the memory of Professor Robert A. Osteryoung (1927−2004); one of the good guys.

* Author to whom correspondence should be addressed. E-mail: chefvb@buffalo.edu. Phone: (716) 645-6800 ext. 2162. Fax: (716) 645−6963.

(1) Schnabel, R.; Langer, P. *J. Chromatogr.* **1991**, *544*, 137−46.
(2) Santano, E.; Pinto del Carmen, M.; Macias, P. *Enzyme Microb. Technol.* **2002**, *30*, 639−46.
(3) Nakai, Y.; Yamamoto, K.; Terada, K.; Ichikawa, J. *Chem. Pharm. Bull.* **1985**, *32*, 4566−71.
(4) Takaharu, M.; Akira, M. *Anal. Biochem.* **1977**, *83*, 216−21.
(5) Kosmulski, M.; Szczypa, J. *J. Radioanal. Nucl. Chem.* **1990**, *144*, 73−7.
(6) Rappoli, B. J.; Rowley, D. A. *J. Colloid Interface Sci.* **2000**, *226*, 218−1.
(7) Tartakovsky, A.; Drutis, D. M.; Carnali, J. O. *J. Colloid Interface Sci.* **2003**, *263*, 408−19.
(8) Göbölös, S.; Tálas, E.; Hegedüs, M.; Bertóti, I.; Margitfalvi, J. L. *Appl. Catal., A* **1997**, *152*, 63−8.
(9) Heckel, A.; Seebach, D. *Chem. Eur. J.* **2002**, *8*, 559−72.
(10) Pluym, B.; Slegers, G.; Claeys, A. *Enzyme Microb. Tech.* **1988**, *10*, 656−9.
(11) Freel-Meyers, C. L.; Borch, R. F. *Org. Lett.* **2003**, *5*, 341−4.
(12) Thaden, J.; Miller, P. S. *Bioconjugate Chem.* **1993**, *4*, 395−401.
(13) Adinolfi, M.; Barone, G.; De Napoli, L.; Iadonisi, A.; Piccialli, G. *Tetrahedron Lett.* **1998**, *39*, 1953−6.
(14) Saari, L. A.; Seitz, W. R. *Anal. Chem.* **1982**, *54*, 823−4.
(15) Vidal, M.; Prata, M.; Santos, S.; Tavares, T.; Oliva, A.; Hossfeld, J.; Preininger, C. *Analyst* **2000**, *125*, 1387−91.
(16) Mulchandani, P.; Chen, W.; Mulchandani, A. *Environ. Sci. Technol.* **2001**, *35*, 2562−5.
(17) Rosa, C. C.; Cruz, H. J.; Vidal, M.; Oliva, A. G. *Biosens. Bioelectron.* **2002**, *17*, 45−52.
(18) Lee, H.; Young Ah, K.; Young Ae, C.; Yong Tae, L. *Chemosphere* **2002**, *46*, 571−6.
(19) Unger, K. K. *Porous Silica*. Elsevier Scientific Pub. Co.: New York, 1979.
(20) Kirkland, J. J.; Dilks, C. H., Jr.; DeStefano, J. J. *J. Chromatogr.* **1993**, *635*, 19−30.
(21) Bieganowska, M. L.; Petruczynik, A. *Chromatographia* **1996**, *43*, 654−8.
(22) Mifune, M.; Mori, Y.; Onoda, M.; Iwado, A.; Motohashi, N.; Haginaka, J.; Saito, Y. *Anal. Sci.* **1998**, *14*, 1127−31.
(23) Sessler, J. L.; Král, V.; Genge, J. W.; Thomas, R. E.; Iverson, B. L. *Anal. Chem.* **1998**, *70*, 2516−22.
(24) Suzuki, Y.; Quina, F. H.; Berthod, A.; Williams, R. W., Jr.; Culha, M.; Mohammadzai, I. U.; Hinze, W. L. *Anal. Chem.* **2001**, *73*, 1754−65.
(25) Nenoff, T. M.; Showalter, M. C.; Salaz, K. A. *J. Mol. Catal. A: Chem.* **1997**, *121*, 123−9.

10.1021/la0490184 CCC: $27.50 © 2004 American Chemical Society
Published on Web 10/19/2004

immobilization[30,31] to name but a few applications. The ease with which one can immobilize a wide array of "ligands" onto silica through the aminopropyl group contributes to the common use of aminopropyl-modified silica. Given this, it is not surprising to learn that a number of spectroscopic techniques have been used to study aminopropyl-modified silica. For example, NMR,[32−34] IR,[35] Raman,[36,37] photoacoustic,[38,39] and X-ray photoelectron[40] spectroscopies have been used to determine the extent of derivatization, the bonding chemistry, and the distribution and structure of surface-bound ligands on aminopropyl-modified silicas.

Fluorescence spectroscopy is an attractive tool for investigating interfaces. The use of fluorescence to characterize silica surfaces is well documented, especially silica-based materials that have importance to chromatography. Specifically, fluorescence-based experiments on either covalently attached[41−53] or physiosorbed probe molecules[54−62] have been carried out to gain a better understanding of the orientation, distribution, mobility, and accessibility of surface-bound ligands.

The current work focuses on determining the effects of a probe molecule's loading, solvent dipolarity, and surface-residue end capping on the cybotactic region that surrounds a covalently attached organic probe molecule on aminopropyl CPG. In previous work, researchers have typically investigated the effects of a covalently attached probe molecule when the probe molecule loading ranged from 0.13 to 1.10 μmol/g.[43−46] In previous studies where the fluorescent probe is covalently attached to pre-aminated silica, a typical probe-to-amine ratio was on the order of 0.5:1.[41,42] In the current work, the probe-to-amine ratio spans 5 orders of magnitude; a much larger range in comparison to those investigated previously.[41−53]

Dansyl was chosen as our probe molecule because an amine-selective analogue (dansyl-SO_2Cl) is commercially available, it is reasonably fluorescent, and its emission spectrum is solvatochromic. Thus, changes in the physicochemical properties surrounding the dansyl probe are reflected in its emission spectrum. Dansyl has also been used previously as a probe to study silica,[41,42,61] glass fibers,[63,64] polymeric films,[65,66] and sol−gel-derived xerogels.[67] Three dansyl-based subsystems were studied in the current work (Figure 1): (a) dansylpropylsulfonamide (DPSA)—the free probe, (b) dansyl covalently attached to aminopropyl-controlled pore glass (D-CPG), and (c) D-CPG derivatized with trimethylchlorosilane (silanized D-CPG). The DPSA experiments serve as a benchmark to determine how the probe itself is solvated in the absence of CPG. The D-CPG experiments were carried out to determine how the cybotactic region that is sensed by the dansyl reporter groups are modulated by (1) the molar ratio of dansyl to amine (D/A) and (2) the solvent dipolarity. The D-CPG is porous and consists of dansyl, free aminopropyl groups ($-C_3H_6-NH_2$) that did not react with dansyl-SO_2-Cl, residual silanol groups ($Si-(OH)_x$), and the silicon dioxide backbone (O−Si−O). The silanized D-CPG experiments provided a system where the majority of free amine and silanol groups are capped with trimethyl silyl groups ($-Si-(CH_3)_3$); thus, silanized D-CPG consists of pores, dansyl, trimethyl silylamine ($-NH-Si-(CH_3)_3$), trimethyl siloxane ($-O-Si-(CH_3)_3$), free aminopropyl and silanol groups that did not react with trimethylchlorosilane, and the silicon dioxide backbone.

Experimental Section

Chemicals and Reagents. Aminopropyl-CPG was purchased from CPG, Inc. (now Millipore). The following characteristics are reported by the vendor: particle size, 34−74 μm; mean pore diameter, 182 Å; surface area, 113 m^2/g; and surface amine concentration, 701.9 μmol/g. Dansyl chloride (98%) was purchased from Aldrich and used without further purification. All solvents were from Sigma-Aldrich (HPLC, 99.8+%). Acetonitrile and toluene were distilled from calcium hydride and stored over 4-Å molecular sieves (Aldrich) prior to use. Triethylamine and pyridine were also dried over 4-Å molecular sieves before use. Trimethylchlorosilane was purchased from Aldrich (98+%) and used without further purification.

(26) Tamami, B.; Iranpoor, N.; Mahdavi, H. *Synth. Commun.* **2002**, *32*, 1251−8.
(27) Macquarrie, D. J.; Maggi, R.; Mazzacani, A.; Sartori, G.; Sartorio, R. *Appl. Catal., A* **2003**, 183−8.
(28) Reynhardt, J. P. K.; Alper, H. *J. Org. Chem.* **2003**, *68*, 8353−60.
(29) Ayadim, M.; Habib Jiwan, J. L.; De Silva, A. P.; Soumillion, J. Ph. *Tetrahedron Lett.* **1996**, *37*, 7039−42.
(30) Ong, S.; Cal, S. J.; Bernal, C.; Rhee, D.; Qiu, X.; Pidgeon, C. *Anal. Chem.* **1994**, *66*, 782−92.
(31) Haddleton, D. M.; Duncalf, D. J.; Kukulj, D.; Radigue, A. P. *Macromolecules* **1999**, *32*, 4769−75.
(32) Sudoelter, E. J. R.; Huis, R.; Hays, G. R.; Nicoletta, A. C. M. *J. Colloid Interface Sci.* **1985**, *103*, 554−60.
(33) Caravajal, G. S.; Leyden, D. E.; Quinting, G. R.; Maciel, G. E. *Anal. Chem.* **1988**, *60*, 1776−86.
(34) Albert, K.; Brindle, R.; Schmid, J.; Buszewski, B.; Bayer, E. *Chromatographia* **1994**, *38*, 283−90.
(35) Seiichi, K.; Ishikawa, T.; Yamagami, N.; Kiyotaka, Y.; Yoshiko, N. *Bull. Chem. Soc. Jpn.* **1987**, *60*, 95−7.
(36) Shimizu, I.; Okabayashi, H.; Taga, K.; Yoshino, A.; Nishio, E.; O'Conner, C. J. *Vib. Spectrosc.* **1997**, *14*, 125−32.
(37) Davis, C. A.; Graves, P. R.; Healy, P. C.; Myhra, S. *Appl. Surf. Sci.* **1993**, *72*, 419−26.
(38) Lochmüller, C. H.; Wilder, D. R. *Anal. Chim. Acta* **1980**, *118*, 101−8.
(39) Urban, M. W.; Koenig, J. L. *Appl. Spectrosc.* **1986**, *40*, 513−9.
(40) Kallury, K. M. R.; Krull, U. J.; Thompson, M. *Anal. Chem.* **1988**, *60*, 169−72.
(41) Lochmüller, C. H.; Marshall, D. B.; Wilder, D. R. *Anal. Chim. Acta* **1981**, *130*, 31−43.
(42) Lochmüller, C. H.; Marshall, D. E.; Harris, J. M. *Anal. Chim. Acta* **1981**, *131*, 263−9.
(43) Lochmüller, C. H.; Colborn, A. S.; Hunnicutt, M. L.; Harris, J. M. *Anal. Chem.* **1983**, *55*, 1344−8.
(44) Lochmüller, C. H.; Colborn, A. S.; Hunnicutt, M. L.; Harris, J. M. *J. Am. Chem Soc.* **1984**, *106*, 4077−82.
(45) Lochmüller, C. H.; Hunnicutt, M. L. *J. Phys. Chem.* **1986**, *90*, 4318−22.
(46) Lochmüller, C. H.; Kersey, M. T. *Anal. Chem.* **1988**, *60*, 1910−4.
(47) Wong, A. L.; Hunnicutt, M. L.; Harris, J. M. *Anal. Chem.* **1991**, *63*, 1076−81.
(48) Wong, A. L.; Hunnicutt, M. L.; Harris, J. M. *J. Phys. Chem.* **1991**, *95*, 4489−95.
(49) Wong, A. L.; Harris, J. M. *J. Phys. Chem.* **1991**, *95*, 5895−901.
(50) Zilberstein, J.; Bromberg, A.; Berkovic, G. *J. Photochem. Photobiol. A* **1994**, *77*, 69−81.
(51) Wang, H.; Harris, J. M. *J. Am. Chem. Soc.* **1994**, *116*, 5754−61.
(52) Wang, H.; Harris, J. M. *J. Phys. Chem.* **1995**, *99*, 16999−17009.
(53) Bartels, M. J.; Koeberg, M.; Verhoeven, J. W. *Eur. J. Org. Chem.* **1999**, 2391−5.
(54) Bauer, R. K.; Borenstein, R.; de Mayo, P.; Okada, K.; Rafalska, M.; Ware, W. R.; Wu, K. C. *J. Am. Chem. Soc.* **1982**, *104*, 4635−44.
(55) Bauer, R. K.; de Mayo, P.; Okada, K.; Ware, W. R.; Wu, K. C. *J. Phys. Chem.* **1983**, *87*, 460−6.
(56) Ståhlberg, J.; Almgren, M. *Anal. Chem.* **1985**, *57*, 817−21.
(57) Avnir, D.; Busse, R.; Ottolenghi, M.; Wellner, E.; Zachariasse, K. A. *J. Phys. Chem.* **1985**, *89*, 3251−6.
(58) Carr, J. W.; Harris, J. M. *Anal. Chem.* **1986**, *58*, 626−31.
(59) Carr, J. W.; Harris, J. M. *Anal. Chem.* **1987**, *59*, 2546−50.
(60) Ståhlberg, J.; Almgren, M., Alsins, J. *Anal. Chem.* **1988**, *60*, 2487−93.
(61) Men, Y.; Marshall, D. B. *Anal. Chem.* **1990**, *62*, 2606−12.
(62) Lochmüller, C. H.; Wenzel, T. J. *J. Phys. Chem.* **1990**, *94*, 4230−5.
(63) Gonzalez-Benito, J.; Cabanelas, J. C.; Aznar, A. J.; Vigil, M. R.; Bravo, J.; Baselga, J. *J. App. Polym. Sci.* **1996**, *62*, 375−84.
(64) Gonzalez-Benito, J.; Aznar, A.; Baselga, J. *J. Fluorescence* **2001**, *11*, 307−14.
(65) Holmes-Farley, S. R.; Whitesides, G. M. *Langmuir* **1986**, *2*, 266−81.
(66) Shea, K. J.; Sasaki, D. Y.; Stoddard, G. J. *Macromolecules* **1989**, *22*, 1722−30.
(67) Pandey, S.; Baker, G. A.; Kane, M. A.; Bonzagni, N. J.; Bright, F. V. *Chem. Mater.* **2000**, *12*, 3547−51.

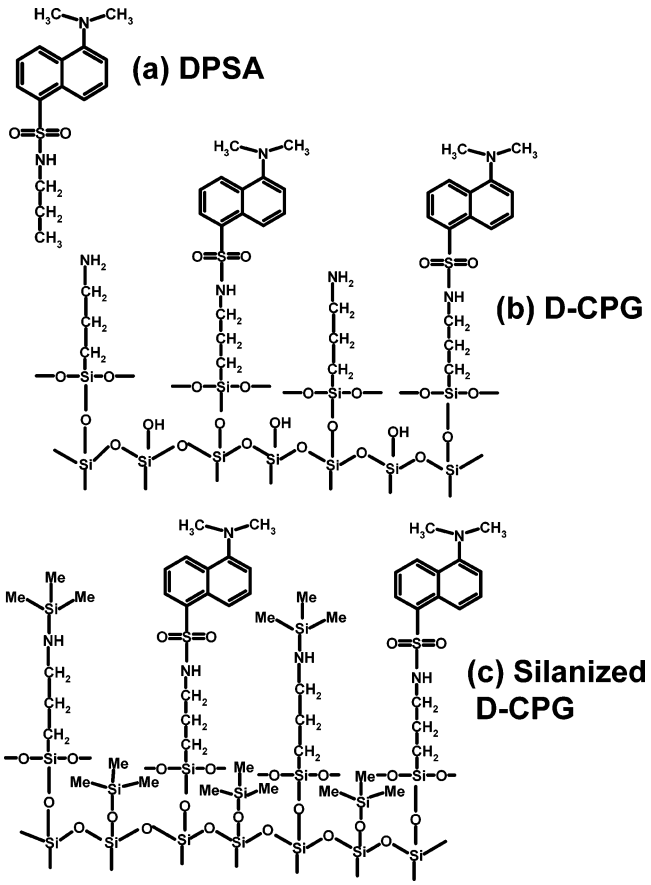

Figure 1. The system under study. Chemical structures for (a) dansylpropylsulfonamide (DPSA), (b) unsilanized dansyl-labeled controlled pore glass (D-CPG), and (c) silanized dansyl-labeled controlled pore glass (silanized D-CPG).

Dansylpropylsulfonamide (DPSA) Synthesis. Dansyl chloride was reacted under ambient conditions with a 25-fold molar excess of propylamine for a period of 1 week at room temperature in the dark. Residual propylamine was removed by evaporation with a stream of N_2, leaving behind crude DPSA. The crude DPSA was subsequently purified by column chromatography.

Dansyl-Labeled Controlled Pore Glass (D-CPG) Synthesis. In a typical reaction, 0.5 g of aminopropyl-CPG was added to 30 mL of dry acetonitrile under Ar(g) in a dry round-bottom flask. An appropriate amount of dansyl chloride (to achieve a desired D/A) was then dissolved in dry acetonitrile and slowly introduced into the flask via a syringe. After adding all the dansyl, 2 equiv of dry triethylamine were then added to the reaction mixture and the reaction flask was heated to 50 °C for 24 h under dry Ar (g). The dansylated particles were then exhaustively washed with acetonitrile, ethanol, hexane, and water until the washings exhibited no detectable dansyl fluorescence. The labeled particles were dried in a vacuum oven for several hours at 70 °C to remove residual solvent.

To confirm that this washing protocol removed all nonspecifically adsorbed dansyl molecules from the aminopropyl-CPG, virgin aminopropyl-CPG particles were incubated for several hours in a solution of DPSA in acetonitrile (molar ratio of DPSA to amine = 2). These particles were then washed with the same series of solvents that we used for the dansylated particles, and the fluorescence of these particles was compared to the aminopropyl-CPG blanks. The results of these experiments showed that all nonspecifically adsorbed dansyl was successfully removed by our washing protocol.

Dansyl Surface Concentration. The dansyl loading on the CPG was controlled by preparing separate batches of dansylated particles as described above with different molar ratios of dansyl-SO_2Cl to CPG amine. The actual D/A values for the dansylated particles were determined by mass balance. Specifically, after a given reaction, we carefully determined *all* the residual dansyl fluorescence in the reaction solution and each washing solution. We then used a series of dansyl calibration curves in each solvent to determine the total concentration of residual dansyl. From the known dansyl concentration that we loaded into the reaction solvent, we determined the concentration of dansyl molecules that were attached to a particular set of CPG particles. The dansyl detection limits were on the order of 6 pM, a concentration at least 3 orders of magnitude below any dansyl concentration used in any reaction. The resulting D/A values for a given set of reaction conditions are presented in Table 1. The imprecision in these D/A values is <4% RSD.

Table 1. CPG Dansyl Surface Loadings (D/A) as a Function of Reaction Conditions

molar ratio of dansyl-SO_2Cl to total CPG amines in the reaction mixture	final CPG D/A
10	0.59
1	0.32
0.1	0.1
10^{-2}	10^{-2}
10^{-3}	10^{-3}
10^{-4}	10^{-4}
10^{-5}	10^{-5}

Preparation of Silanized D-CPG. D-CPG was dried in a vacuum oven for several hours at 70 °C. In a typical reaction, 0.25 g of a particular D-CPG sample (specific D/A) was added to 30 mL of dried toluene under dry Ar (g) in a presilanized dry round-bottom flask equipped with a magnetic stirrer and reflux column. Trimethylchlorosilane (5 mL) was then added to the reaction flask, followed by 2 mL of dry pyridine, and the contents were refluxed for 24 h under dry Ar (g). The silanized particles were then thoroughly washed with ethanol, hexane, and toluene to remove unreacted silane. These particles were subsequently dried in a vacuum oven for several hours at 70 °C.

Dansyl molecules were not detected in these washing solutions, showing that silanization did not liberate any detectable dansyl molecules from the CPG.

Fluorescence Measurements. All particles were placed in a vacuum oven at 70 °C for at least 1 h before they were used for study. The particles for study were then loaded into clean 1.5-mm diameter quartz capillary tubes (Technical Glass, Inc.). Each sample-loaded capillary was immersed in a given solvent contained within a filter flask. Vacuum was applied to the flask, air was removed from around the particles, and the solvent was drawn fully into the capillary, thus solvating the particles. The particles were allowed to equilibrate with the solvent for approximately 15 min before any fluorescence measurements were conducted. Separate capillaries were prepared for each sample/solvent combination. The fluorescence spectra for a given sample in a particular solvent did not change more than 3% over three months.

Fluorescence spectra were recorded by using an SLM-AMINCO model 8100. A 450 W Xe arc lamp was used for the excitation source. Double- and single-grating monochromators served as the excitation and emission wavelength selection devices, respectively. The excitation wavelength was maintained at 342 nm. The excitation and emission spectral band-passes were maintained at 2 and 4 nm, respectively, for all experiments. All emission spectra were background corrected by using appropriate blanks. The blank contribution was always <2% of the total emission.

All experiments were performed on at least three occasions. Average results are reported along with the corresponding measurement standard deviations.

Analysis of the Steady-State Emission Spectra. In most of our experiments, the observed steady-state emission spectra *appear* as a single peak. However, when we investigated the D/A = 10^{-4} particles, it became clear that each spectrum (vide infra) resulted from the superposition of multiple emission spectra. Given this, all of our spectra under all conditions were considered to arise from dansyl molecules that were simultaneously emitting from different microenvironments. We used PeakFit (Jandel Scientific) to deconvolve each observed spectrum into the spectra from the individual dansyl molecular microenvironments. For

the high ($>10^{-3}$) and low (10^{-5}) D/A particles, the observed emission resulted from one major emissive species. In the D/A = 10^{-4} particles, the dansyl molecules are emitting simultaneously from at least two different microenvironments. The emission maximum for one of the deconvolved spectra was solvent dependent (lower-energy emission). The emission maximum for the second deconvolved spectrum was solvent independent (higher-energy emission).

Theory. The Lippert−Mataga expression (eq 1) provides a link between the observed spectral shift and a solvent's physicochemical properties:[68]

$$\bar{\nu}_A - \bar{\nu}_F = \frac{2}{hc}\left(\frac{\epsilon - 1}{2\epsilon + 1} - \frac{n^2 - 1}{2n^2 + 1}\right)\frac{(\mu_E - \mu_G)^2}{a^3} + \text{constant} \quad (1)$$

In this expression, ν_A and ν_F represent the absorbance and emission maximum (cm^{-1}), respectively, h is Plank's constant, c is the speed of light, a is the radius swept out by the fluorophore, μ_E and μ_G are the fluorophore's excited and ground-state dipole moments, respectively, and ϵ and n denote the solvent dielectric constant and refractive index, respectively. The term that is a function of ϵ and n is collectively called the orientation polarizability, symbolized by ΔF. ΔF accounts for the spectral shift resulting from the redistribution of "solvent" molecules that surround the fluorophore. Hence, the Lippert−Mataga expression provides an important relationship between a solvatochromic fluorophore's emission spectrum and the physical properties of the fluorophore's cybotactic region.

All of our Lippert−Mataga plots were constructed by using the emission maxima associated with the lowest-energy emission spectra (vide supra).

Results and Discussion

Steady-State Fluorescence from DPSA in Liquids, Unsilanized D-CPG, and Silanized D-CPG in Air. The dansyl excitation/absorbance spectra are generally not too solvent dependent (results not shown).[41,42,61,63−67] Figure 2 presents typical steady-state emission spectra from DPSA dissolved in several organic liquids (Figure 2A) along with spectra from unsilanized D-CPG (Figure 2B) and silanized D-CPG (Figure 2C) in air as a function of D/A. Inspection of these results reveals several important trends. The DPSA emission maximum shifts from 444 nm in hexane to 515 nm in methanol (Figure 2A), a difference in energy of ~3100 cm^{-1}, illustrating the solvatochromic behavior of the free dansyl molecules. The D-CPG emission maximum in air (Figure 2B) red shifts from 420 nm when the CPG is sparingly dansylated (D/A = 10^{-5}) to 494 nm at the highest D/A studied (0.6), a difference in energy of ~3600 cm^{-1}. This result shows that the dansyl groups attached to the CPG particles encounter cybotactic regions that depend strongly on D/A. Specifically, one can tune the dipolarity sensed by the dansyl groups attached to CPG to a substantially greater extent by adjusting the D/A in comparison to changing the solvent that surrounds DPSA from hexane to methanol. When the D/A is high, the dansyl reporter groups sense a very dipolar microenvironment; the emission maximum from the D/A = 0.6 D-CPG is comparable to that of DPSA dissolved in liquid 1-butanol. However, when the D/A is low (10^{-5}), the dansyl reporter groups are distributed into microenvironments that *appear* less dipolar than sensed by DPSA dissolved in liquid hexane.

The results for silanized D-CPG (Figure 2C) are similar in comparison to unsilanized D-CPG; however, the emission maxima do not systematically blue shift with decreasing D/A. The silanized D-CPG emission maximum in air red shifts from 420 nm when the CPG is sparingly dansylated (D/A = 10^{-5}) to 482 nm at the highest D/A (0.6), a difference in energy of ~3100 cm^{-1}. However, the emission maxima for the particles with a D/A of 0.6 to 10^{-3} are very similar to one another, indicating that these dansyl groups are sensing a similar dipolarity over this D/A range. Thus, the dipolarity sensed by the dansyl reporter groups on silanized D-CPG is more constant/uniform over a much larger D/A range in comparison to that observed for the corresponding unsilanized D-CPG particles.

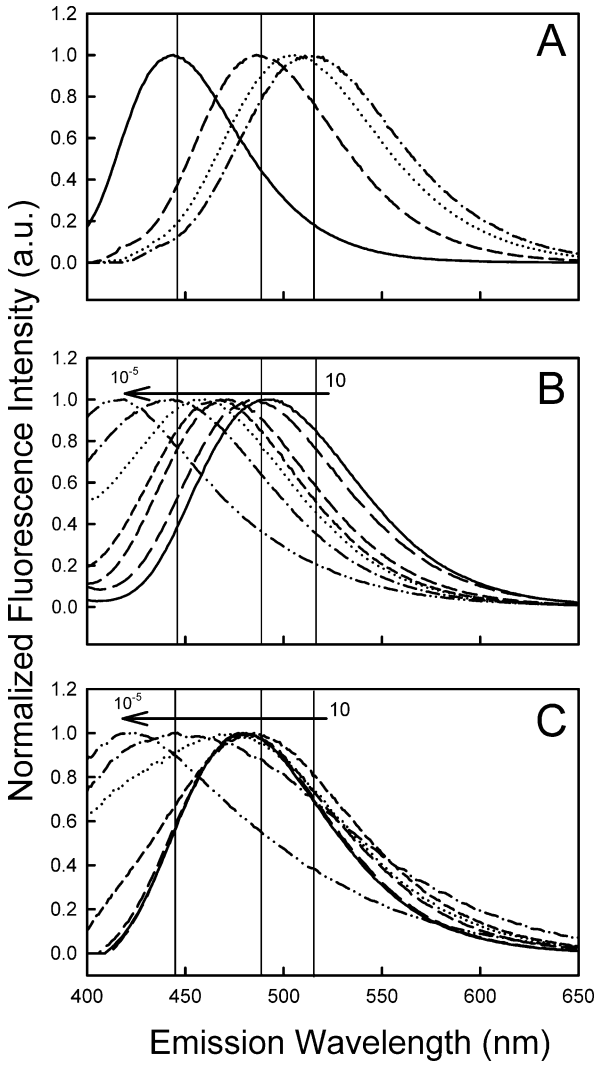

Figure 2. Normalized steady-state emission spectra for various dansylated species. (Panel A) DPSA dissolved in several liquid organic solvents. (Panel B) D/A-dependent spectra for unsilanized D-CPG in air. (Panel C) D/A-dependent spectra for silanized D-CPG in air. Symbols: (Panel A) hexane (—), ethyl acetate (– – –), 1-butanol (· · ·), and methanol (– · –). (Panels B and C) D/A = 0.6 (—), 0.3 (— — —), 0.1 (– – –), 10^{-2} (- - -), 10^{-3} (· · ·), 10^{-4} (– · –), and 10^{-5} (– ·· –). The three vertical lines are aids to the reader's eye to help assess differences in the spectra. They mark the emission maxima of DPSA in (left to right) hexane, ethyl acetate, and methanol.

Lippert−Mataga Analysis of DPSA, Unsilanized D-CPG, and Silanized D-CPG in Contact with Liquids. Figure 3 presents the solvent- and D/A-dependent Lippert−Mataga plots for unsilanized D-CPG (Figure 3A) and silanized D-CPG (Figure 3B). Recall that these plots are constructed from the red-most spectral features in the steady-state emission spectra (vide supra). Results for DPSA are also shown in each panel (- - -). Figure 4 summarizes and compares the Lippert−Mataga plots

(68) Lakowicz, J. R. *Principles of Fluorescence Spectroscopy*, 2nd ed.; Plenum Press: New York, 1999; Chapters 6 and 7.

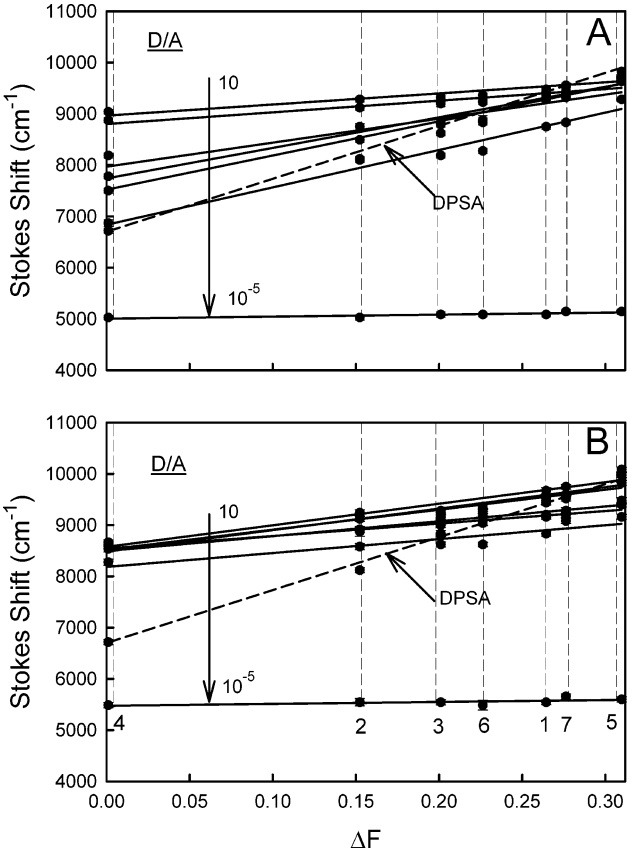

Figure 3. D/A-dependent Lippert−Mataga plots for unsilanized and silanized D-CPG. DPSA results are also shown in each Panel (- - -). (Panel A) Unsilanized D-CPG. (Panel B) Silanized D-CPG. The solvents are: (1) 1-butanol, (2) chloroform, (3) ethyl acetate, (4) hexane, (5) methanol, (6) 1-octanol, and (7) 1-propanol.

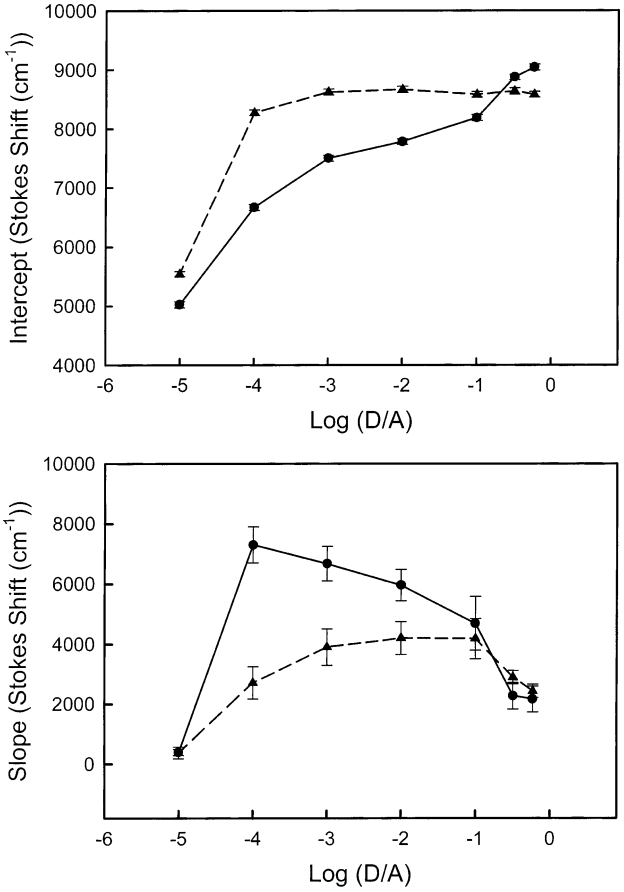

Figure 4. Summary of the data presented in Figure 3. Unsilanized (—) and silanized D-CPG (- - -). (Panel A) Lippert−Mataga plot intercepts. (Panel B) Lippert−Mataga plot slopes.

(Figure 3) by presenting the unsilanized D-CPG (—) and silanized D-CPG (- - -) intercepts (Figure 4A) and slopes (Figure 4B). The intercept values provide a measure of the local dipolarity sensed by the dansyl reporter groups in the absence of any solvent. The slope values indicate the sensitivity/susceptibility of the dansyl reporter groups to solvent. The results on unsilanized D-CPG show that D/A has a substantial affect on the cybotactic region surrounding the dansyl moieties. The D/A does not have such a large affect on the silanized D-CPG particles (Figure 3B). The Lippert−Mataga plot slopes for the CPG particles never exceed the value for DPSA, indicating that the dansyl reporter groups that are attached to CPG are never as solvent sensitive/susceptible in comparison to free DPSA molecules in solution.

The results for unsilanized D-CPG (—) show that the intercept values (Figure 4A) systematically decrease with decreasing D/A. The corresponding results for silanized D-CPG (- - -) indicate that the intercept values remain nearly constant between D/A = 0.6 and 10^{-4}. The intercept values then decrease for the lowest D/A (10^{-5}) on both types of CPG particles. The unsilanized D-CPG (—) slope results (Figure 4B) indicate that, at high D/A (0.6 and 0.3), the slope is small but the slope then systematically increases as the D/A decreases to 10^{-4}. The slope then plummets for the particles with a D/A of 10^{-5}. The results for silanized D-CPG (- - -) show that, at high D/A, the slope is small and similar to that of the D/A = 0.6 and 0.3 unsilanized D-CPG particles. As D/A is decreased, the slope increases and remains essentially constant between D/A = 0.1 and 10^{-3}. The slope then decreases for the particles with a D/A of 10^{-4} and then plummets for the 10^{-5} particles to a value similar to that seen for the unsilanized D-CPG 10^{-5} particles.

Interpretation of the Unsilanized D-CPG Results. The D/A-dependent unsilanized D-CPG Lippert−Mataga plot data can be interpreted by considering that the overall orientation polarizability sensed by the dansyl reporter groups on the unsilanized CPG particles, $\Delta F_{\text{observed,un}}$, arises from the contribution of multiple species:

$$\Delta F_{\text{observed,un}} = P_{\text{SiOH}}C_{\text{SiOH}}\Delta F_{\text{SiOH}} + P_{\text{NH}_2}C_{\text{NH}_2}\Delta F_{\text{NH}_2} + P_{\text{SiO}_2}C_{\text{SiO}_2}\Delta F_{\text{SiO}_2} + P_{\text{Dan}}C_{\text{Dan}}\Delta F_{\text{Dan}} + P_{\text{solvent}}C_{\text{solvent}}\Delta F_{\text{solvent}} \quad (2)$$

In this expression, ΔF_x represents the orientational polarizability terms arising from the solvent and the various functional groups on the D-CPG. Representative estimates of ΔF_x are collected in Table 2.[69−74] The P_x terms

(69) The ΔF of dansyl was determined by measuring the Stokes shift of solid DPSA and extrapolating the ΔF value on the linear regression line of the DPSA Lippert plot.

(70) Lide, D. R., Ed. *Handbook of Chemistry and Physics*; CRC Press: Boca Raton, 2004.
(71) Grubb, W. T.; Osthoff, R. C. *J. Am. Chem. Soc.* **1953**, *75*, 2230−2.
(72) Cook, R. L.; Mills, A. P. *J. Phys. Chem.* **1961**, *65*, 252−4.
(73) Willey, G. R. *J. Phys. Chem.* **1967**, *71*, 4294−8.
(74) Freiser, H.; Eagle, M. V.; Speier, J. *J. Am. Chem. Soc.* **1952**, *75*, 2824−7.

Table 2. Estimated Orientational Polarizability (ΔF) for the Various Groups on the Unsilanized and Silanized D-CPG Particles

group	ΔF
dansyl	0.22[a]
$CH_3CH_2CH_2\mathbf{NH_2}$	0.18[b]
$(CH_3)_3$−Si-**OH**	0.21[c]
SiO_2	0.11[d]
CH_3CH_2−NH-**Si**−$\mathbf{(CH_3)_3}$	0.037[e,f]
$\mathbf{CH_3CH_2}$ −**O**-Si -$(CH_3)_3$	0.046[g]

[a] Reference 69. [b] Reference 70. [c] Reference 71. [d] Reference 70. [e] Reference 72. [f] Reference 73. [g] Reference 74.

represent a proximity term relating the closeness of the dansyl reporter groups to solvent or functional group x. The C_x terms represent the corresponding fractional contributions of $x(\Sigma C_x = 1)$. At high D/A (i.e., 0.6 and 0.3), the dansyl reporter groups are in the most dipolar environment and not particularly solvent sensitive. Since these CPG particles are rich with dansyl groups, C_{Dan} is the dominate term and it contributes the most to $\Delta F_{observed,un}$. This result is consistent with dansyl molecules having the largest ΔF value (0.22) in comparison to any of the other D-CPG functional groups. In addition, at high D/A, the dansyl groups are "solvated" by other, dipolar dansyl molecules and the addition of dipolar solvents can only slightly augment the dipolarity that surrounds these dansyl groups.

As we lower the D/A from 0.1 to 10^{-4}, the dipolarity sensed by the dansyl reporter groups decreases and the dansyl reporter groups become more solvent sensitive/susceptible. The former result can be explained by the fact that, as D/A decreases, the number of free aminopropyl groups systematically increases while the number of "local" dansyl groups decreases, causing C_{Dan} to decrease and C_{NH_2} to increase. Thus, the dansyl moieties sense more of the free aminopropyl groups ($\Delta F = 0.18$) and, consequently, encounter a less dipolar environment in comparison to the D/A = 0.6 and 0.3 particles. The latter result is consistent with the average distance between dansyl reporter groups increasing, solvent accessing/solvating/wetting the dansyl groups ($C_{solvent}$ increases), and consequently, altering the cybotactic region surrounding the dansyl reporter groups to a greater extent than that observed for the D/A = 0.6 and 0.3 particles. Thus, as we lower D/A from 0.1 to 10^{-4}, the dansyl reporter groups become more sensitive to solvent. The observed increase in solvent sensitivity for the intermediate D/A particles (i.e., 0.1 to 10^{-4}) could arise from dansyl groups that become more accessible to solvent and/or particles or domains with dansyl reporters that become better wetted by the solvents.

Molecules such as dansyl exhibit solvatochromic behavior for at least two reasons.[75−77] First, they exhibit general solvent effects arising from the fluorophore's change in dipole moment upon photoexcitation and the solvent's dielectric constant and refractive index as described by the Lippert−Mataga expression (eq 1). Second, a portion of their solvatochromism can arise from intramolecular interconversion between the locally excited (LE) and the twisted intramolecular charge-transfer (TICT) state. Upon photoexcitation, the less polar, semiplanar LE state forms initially (similar in structure to the ground state). In certain circumstances, the LE state can undergo intramolecular electron transfer from a donor residue (dimethyl amino group in dansyl) to an acceptor group (naphthalene ring in dansyl) with a corresponding twist of the donor residue about the bond that connects it to the acceptor. In the TICT state, the donor and acceptor are orthogonal to one another and this state is more dipolar in comparison to the LE state. Thus, the propensity to form a TICT state and shift the emission spectrum is influenced by the solvent's dielectric properties that help to mediate charge transfer *and* the ability of the donor residue to rotate within the fluorophore. The former is governed primarily by the solvent dielectric properties, and the latter depends also on any physical impediments to donor rotation. We suggest that the dansyl groups in the D/A = 10^{-5} unsilanized D-CPG particles are insensitive to changes in solvent polarity because they are located in a relatively hydrophobic environment (e.g., silicon dioxide, $\Delta F = 0.11$) that is solvent inaccessible *and/or* the dansyl reporter groups are located in a restrictive domain (e.g., small pores) which physically impedes the $-N(CH_3)_2$ group from reorienting and prevents dansyl from forming a TICT state. Thus, the dansyl fluorescence occurs primarily from the higher-energy LE state.

The unsilanized D-CPG results are consistent with three major dansyl sub-populations. One sub-population consists of clusters/islands of surface-bound dansyl molecules in which one dansyl group is surrounded by many other dansyl molecules. The dansyl moieties within these domains are not very solvent sensitive/susceptible because these clusters/islands are saturated with dansyl moieties and the addition of dipolar solvents can only slightly augment the dipolarity that surrounds the dansyl groups. This dansyl subpopulation is populated to the largest degree for the D/A ≥ 0.3 particles. The second dansyl subpopulation consists of more-isolated dansyl molecules on the CPG surface, which, on average, can interact with the various groups (aminopropyl, silanol, and siloxane) on the D-CPG surface more than the dansyl molecules within the dansyl clusters/islands. The relative number of these sites increases as the D/A decreases to ~10^{-4}. As a result, the sensitivity/susceptibility of the dansyl groups to solvent increases with decreasing D/A (0.6 to 10^{-4}) since the average number of these isolated dansyl groups increases over this range. The third dansyl subpopulation consists of dansyl molecules that are "buried" within small CPG pores. These domains are restrictive to dansyl molecule motion and they are relatively solvent inaccessible/insensitive in comparison to the other subpopulations due to their location within the CPG. This subpopulation is the only one that is populated for unsilanized D-CPG at the lowest D/A (10^{-5}).

Interpretation of the Silanized D-CPG Results. Between D/A = 0.6 and 10^{-4}, the silanized D-CPG particle Lippert−Mataga plot intercepts and slopes are, within experimental error, D/A independent. The intercept and slope drop significantly for the D/A = 10^{-5} particles. These results are consistent with the cybotactic region surrounding the dansyl reporter groups not changing significantly with D/A between 0.6 and 10^{-4} for the silanized D-CPG. Thus, the dipolarity sensed by the dansyl reporter molecules on silanized D-CPG appears less heterogeneous as a function of D/A in comparison to the dipolarity on the corresponding unsilanized D-CPG particles. This result is not surprising because any free SiOH or $-NH_2$ groups that become available as D/A is lowered should be silanized, creating a dansyl cybotactic region that would not vary significantly with D/A. Thus, the average "surface" density of groups surrounding a single dansyl moiety does not change as we decrease D/A on silanized D-CPG. This is because, as the number of average dansyl groups decreases, the number of trimethyl silyl groups

(75) Kosower, E. M. *Acc. Chem. Res.* **1982**, *15*, 259−66.
(76) Rettig, W. *Angew Chem., Int. Ed. Engl.* **1986**, *25*, 971−88.
(77) Reichardt, C. *Chem. Soc. Rev.* **1992**, 147−53.

increases, in proportion, keeping the average residue density and overall local dipolarity around any remaining dansyl molecules the same. Thus, although the relative number of isolated dansyl groups increases with decreasing D/A, the average dipolarity and accessibility of the domain that surrounds these dansyl molecules does not appear to change in comparison to the cybotactic region surrounding the dansyl clusters/islands. The behavior of the D/A = 10^{-5} particles is consistent with dansyl molecules located within a relatively hydrophobic environment (e.g., silicon dioxide, $\Delta F = 0.11$) that is solvent inaccessible *and / or* the dansyl reporter groups are located in a restrictive domain (e.g., small pores) that impede the $-N-(CH_3)_2$ residue from reorienting and thus prevents the dansyl molecules from forming a TICT state. In comparison to the unsilanized D-CPG, the microenvironment sensed by the dansyl reporter groups at D/A = 10^{-5} in the silanized D-CPG does not appear to be affected substantially by silanization. Thus, silanization does not appear to significantly modulate the microenvironment surrounding the dansyl residues within D-CPG small pores.

Comparison of Unsilanized and Silanized D-CPG. If we recast eq 2 for the case of silanized CPG and we assume silanization is not 100% efficient, we can write the overall orientation polarizability sensed by the dansyl reporter groups on the silanized CPG particles, $\Delta F_{\text{observed,s}}$, as

$$\begin{aligned}\Delta F_{\text{observed,s}} = {} & P'_{\text{SiOH}}C'_{\text{SiOH}}\Delta F_{\text{SiOH}} + \\ & P_{\text{SiOSi(CH}_3)_3}C_{\text{SiOSi(CH}_3)_3}\Delta F_{\text{SiOSi(CH}_3)_3} + \\ & P'_{\text{NH}_2}C'_{\text{NH}_2}\Delta F_{\text{NH}_2} + \\ & P_{\text{NHSi(CH}_3)_3}C_{\text{NHSi(CH}_3)_3}\Delta F_{\text{NHSi(CH}_3)_3} + \\ & P_{\text{SiO}_2}C_{\text{SiO}_2}\Delta F_{\text{SiO}_2} + \\ & P_{\text{Dan}}C_{\text{Dan}}\Delta F_{\text{Dan}} + \\ & P'_{\text{solvent}}C'_{\text{solvent}}\Delta F_{\text{solvent}} \end{aligned} \quad (3)$$

The ′ mark is used here to remind the reader that these terms are *not* necessarily the same in eqs 2 and 3 at a given D/A. For example, the proximity to which solvent molecules can approach the dansyl reporter groups or wet the CPG will be affected by the silanization process, thus, the P_{solvent} terms in the unsilanized and silanized D-CPG at a given D/A are likely different. Similarly, any residual free silanols or amines on the silanized D-CPG are likely to be in a different proximity to the dansyl groups in comparison to unsilanized D-CPG even though they are the same chemical species. Figure 5 summarizes the *differences* ($U - S$) between the unsilanized and silanized D-CPG Lippert−Mataga plots. Panels A and B of Figure 5 present the D/A-dependent results for the intercepts and slopes, respectively.

Figure 5A shows several interesting trends. First, at high D/A, the dipolarity sensed by the dansyl reporter groups on the unsilanized D-CPG particles exceeds the dipolarity on the corresponding silanized D-CPG particles. Second, as D/A is lowered, this difference lessens. Third, between D/A = 0.3 and 0.1, the dipolarity sensed by the dansyl reporter groups on the silanized D-CPG particles exceeds the dipolarity on the corresponding unsilanized D-CPG particles. Fourth, between D/A = 0.1 and 10^{-4}, we see that dipolarity sensed by the dansyl reporter groups on the silanized D-CPG systematically increases in comparison to the corresponding unsilanized D-CPG particles. Finally, as D/A decreases from 10^{-4} to 10^{-5}, the differences between the particles lessen again; however, the dipolarity sensed by the dansyl reporter groups on the silanized D-CPG particles exceeds the dipolarity on unsilanized D-CPG in the D/A = 10^{-5} particles.

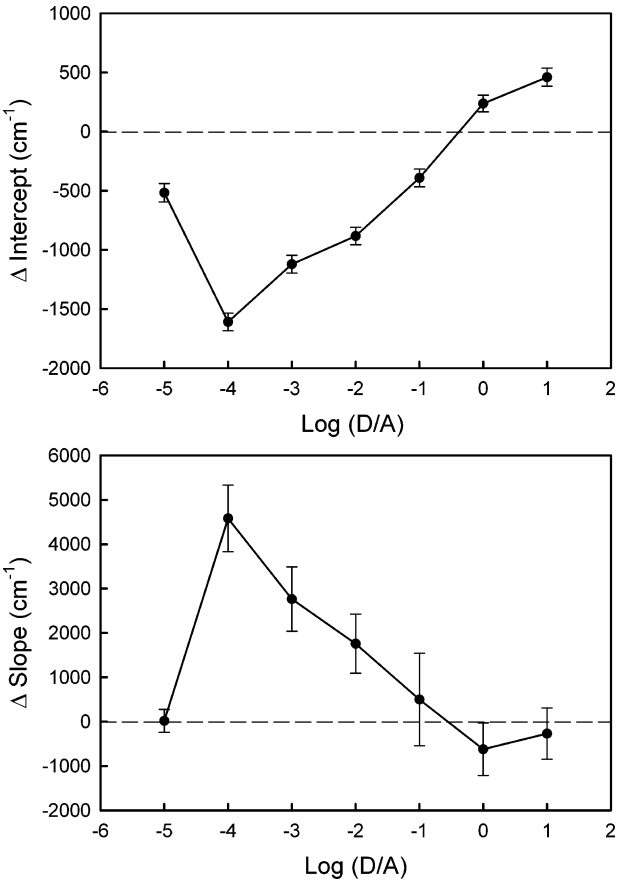

Figure 5. D/A-dependent differences between unsilanized and silanized D-CPG particles. (Panel A) Lippert−Mataga plot intercepts. (Panel B) Lippert−Mataga plot slopes.

Based on eqs 2 and 3 and the estimated ΔF_x terms (Table 2), certain conditions must be met to observe the results reported in Figure 5A. Specifically, to observe a differential intercept ($U - S$) that is *positive*, the following conditions must hold

$$P_{\text{SiOH}}C_{\text{SiOH}}\Delta F_{\text{SiOH}} > [P'_{\text{SiOH}}C'_{\text{SiOH}}\Delta F_{\text{SiOH}} + P_{\text{SiOSi(CH}_3)_3}C_{\text{SiOSi(CH}_3)_3}\Delta F_{\text{SiOSi(CH}_3)_3}] \quad (4a)$$

and/or

$$P_{\text{NH}_2}C_{\text{NH}_2}\Delta F_{\text{NH}_2} > [P'_{\text{NH}_2}C'_{\text{NH}_2}\Delta F_{\text{NH}_2} + P_{\text{NHSi(CH}_3)_3}C_{\text{NHSi(CH}_3)_3}\Delta F_{\text{NHSi(CH}_3)_3}] \quad (4b)$$

and

$$\begin{aligned}[P_{\text{SiOH}}C_{\text{SiOH}}\Delta F_{\text{SiOH}} + P_{\text{NH}_2}C_{\text{NH}_2}\Delta F_{\text{NH}_2}] > {} & \\ [P'_{\text{SiOH}}C'_{\text{SiOH}}\Delta F_{\text{SiOH}} + & \\ P_{\text{SiOSi(CH}_3)_3}C_{\text{SiOSi(CH}_3)_3}\Delta F_{\text{SiOSi(CH}_3)_3} + P'_{\text{NH}_2}C'_{\text{NH}_2}\Delta F_{\text{NH}_2} + & \\ P_{\text{NHSi(CH}_3)_3}C_{\text{NHSi(CH}_3)_3}\Delta F_{\text{NHSi(CH}_3)_3}] & \end{aligned} \quad (4c)$$

This is the situation for the D/A = 0.6 and 0.3 particles.

To observe a differential intercept ($U - S$) that is *negative*, the following conditions must hold

$$P_{SiOH}C_{SiOH}\Delta F_{SiOH} < [P'_{SiOH}C'_{SiOH}\Delta F_{SiOH} + P_{SiOSi(CH_3)_3}C_{SiOSi(CH_3)_3}\Delta F_{SiOSi(CH_3)_3}] \quad (5a)$$

and/or

$$P_{NH_2}C_{NH_2}\Delta F_{NH_2} < [P'_{NH_2}C'_{NH_2}\Delta F_{NH_2} + P_{NHSi(CH_3)_3}C_{NHSi(CH_3)_3}\Delta F_{NHSi(CH_3)_3}] \quad (5b)$$

and

$$[P_{SiOH}C_{SiOH}\Delta F_{SiOH} + P_{NH_2}C_{NH_2}\Delta F_{NH_2}] < [P'_{SiOH}C'_{SiOH}\Delta F_{SiOH} + P_{SiOSi(CH_3)_3}C_{SiOSi(CH_3)_3}\Delta F_{SiOSi(CH_3)_3} + P'_{NH_2}C'_{NH_2}\Delta F_{NH_2} + P_{NHSi(CH_3)_3}C_{NHSi(CH_3)_3}\Delta F_{NHSi(CH_3)_3}] \quad (5c)$$

This is the scenario for the D/A ≤ 0.1 particles.

Taken together, the results in Figure 5A show that silanization, D/A, residue proximity, and solvent access/wetability play off one another and that each can be used to a different degree to tailor the cybotactic region sensed by the dansyl reporter groups attached to CPG.

Inspection of the data in Figure 5B shows that the dansyl reporter group sensitivity/susceptibility to solvent on silanized and unsilanized D-CPG are, within our measurement precision, equivalent for the D/A ≥ 0.1 particles. Between D/A = 10^{-2} and 10^{-4}, the sensitivity/susceptibility of the dansyl reporter groups to solvent lessens for the silanized D-CPG particles in comparison to the corresponding unsilanized D-CPG particles. This result is consistent with silanization augmenting the local dipolarity that is sensed by the dansyl groups such that the dansyl groups are no longer as sensitive to solvent and/or access to the dansyl groups is blocked or otherwise limited by the $-Si(CH_3)_3$ residues. The silanized and unsilanized D-CPG particles at D/A = 10^{-5} behave equally in terms of solvent susceptibility; the dansyl moieties do not sense the solvent. An explanation for this behavior is given above.

A Closer Look at the Dansyl Emission Spectra from the CPG Particles. Leezenberg and Frank[78] observed multiple peaks in the steady-state dansyl emission spectra while studying the precipitation of silica in-situ within end-linked poly(dimethylsiloxane) networks that were labeled with dansyl probes. They assigned the spectral features to multiple dansyl subpopulations. The blue (higher energy) feature in their emission spectrum was attributed to dansyl molecules within a rigid microenvironment, wherein rearrangement of the dansyl molecule's dimethylamino group is impeded and fluorescence occurs from the LE state. The distribution of dansyl molecules within the rigid environment and the mobile network domain (red emission, lower energy), respectively, was reported to determine the fluorescence intensities of the two peaks.

Figure 6 presents a series of normalized steady-state emission spectra from unsilanized D-CPG. Figure 6A presents results in liquid methanol as a function of D/A. Panels B and C of Figure 6 present results at D/A = 10^{-4} and 10^{-5}, respectively, in several organic liquids (varying solvent ΔF). The results in Figure 6A demonstrate that the average dansyl reporter group that emits in the D/A = 0.6 to 10^{-3} unsilanized D-CPG particles senses a dipolar environment ($\lambda_{em} \approx 515$ nm). However, as we proceed to the particles with a D/A = 10^{-4}, two peaks are observed in the emission spectrum, indicating that dansyl molecules are simultaneously reporting from at least two different microenvironments. Deconvolution of the D/A = 10^{-4} spectrum shows that the blue-shifted emission peak is at ~422 nm, while the red-shifted peak appears at ~501 nm. These results indicate that the dansyl reporter groups are located in and reporting from at least two distinct cybotactic regions: one that is nonpolar/restrictive and another that is polar. This general behavior is observed for all the D/A = 10^{-4} particles in each liquid (Figure 6B), indicating that the result is not unique to methanol. [Note:

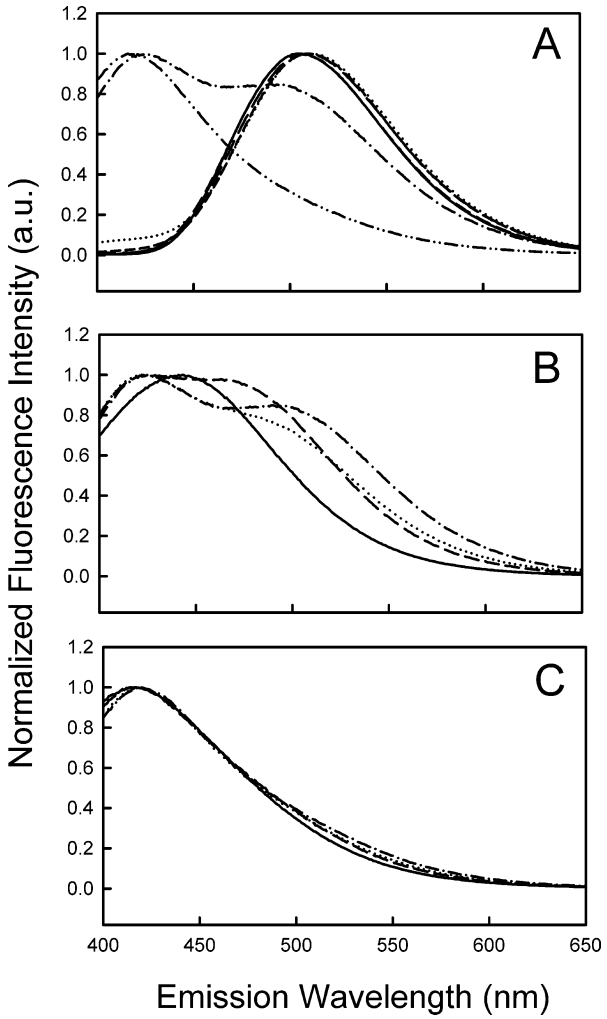

Figure 6. Steady-state emission spectra for unsilanized D-CPG. (Panel A) In liquid methanol at D/A = 0.6 (—), 0.3 (— — —), 0.1 (– – –), 10^{-2} (- - -), 10^{-3} (• • •), 10^{-4} (– • –), and 10^{-5} (– •• –). (Panel B) As a function of solvent at D/A = 10^{-4}. (Panel C) As a function of solvent at D/A = 10^{-5}. The liquids in Panels B and C are hexane (—), ethyl acetate (– – –), 1-butanol (• • •), and methanol (– • –).

Hexane may *appear* to be an exception; however, deconvolution of the observed D/A = 10^{-4} spectrum in hexane shows this *not* to be the case. Specifically, the observed emission spectrum is well fit to a model with two emission spectra. Attempts to fit the spectra to a single spectral feature were always significantly poorer in comparison to the two spectra models. The emission maximum for the blue-deconvolved emission spectrum peaks at 422 nm. The relative emission yield from this bluest-deconvolved emission spectrum is low in compari-

(78) Leezenberg, P. B.; Frank, C. W. *Chem. Mater.* **1995**, *7*, 1784–92.

son to the red-deconvolved emission spectrum. Thus, unlike the results in the other solvents, the contribution to the observed emission from the 422 nm spectrum is much weaker in hexane in comparison to the red spectrum. This result is consistent with the higher quantum yield of dansyl molecules in nonpolar solvents.[79] Finally, the emission maximum for the deconvolved red spectrum in hexane is the most blue of any liquid studied. Thus, the hexane results are not anomalous.]

Deconvolution of all the observed spectra show that the blue spectrum relative contribution to the total emission is a function of D/A and solvent but its emission maximum is solvent independent. The deconvolved red spectrum shifts with solvent ΔF (cf., Figures 3 and 4). These results suggest that the dansyl reporter groups distribute into solvent accessible (red emitting, shifting) and relatively solvent inaccessible/restrictive (blue emitting, no shifting) domains on/within the CPG.

As we proceed to the particles with the lowest D/A (10^{-5}) in methanol, only one peak is observed in the emission spectrum (Figure 6A), suggesting that these dansyl groups are reporting from one microenvironment. This behavior is also evident in the other solvents (Figure 6C), where only one peak is observed and the feature is strongly blue shifted (to ~420 nm) relative to the particles with large D/A values. In addition, the dansyl emission maxima for the D/A = 10^{-5} particles are solvent independent, suggesting that these dansyl molecules are located in a solvent inaccessible or restrictive domain. These dansyl groups may also be distributed in sites that are within narrow pores, which inhibit solvation and/or are restrictive, rather than surrounded by surface sites that actually block or otherwise limit solvent access to the dansyl molecules.

Our results for D-CPG (Figure 6) are consistent with the hypothesis that there are at least two types of *reaction* sites on the aminopropyl CPG for dansyl chloride to form the sulfonamide: (Site 1) a hydrophobic microenvironment (e.g., pore) that is less accessible to solvent and/or restrictive to dansyl molecule's internal dynamics (i.e., LE to TICT formation) and (Site 2) a polar, solvent-accessible domain or ensemble of polar domains. The relative molar ratio of these two site types is such that Site 2 is in much larger concentration in comparison to Site 1. However, Site 1 is much more reactive toward dansyl chloride in comparison to Site 2. Site 2 is consistent with the so-called "strong site" recently described by Wirth[80] and co-workers on Type B silica. Site 1 is reminiscent of island formation following ligand surface migration first described by Wang and Harris.[51] At the low D/A (10^{-5}), the hydrophobic/restrictive site (Site 2) is selectively tagged with dansyl and the emission spectrum consists of a single, blue-shifted peak at ~420 nm that is insensitive to changes in solvent polarity. As the D/A increases, the hydrophobic/restrictive site eventually becomes fully labeled and any further increases in D/A leads to the labeling of the less-reactive and more-polar amine domain(s) (Site(s) 1). This is most obvious in the D/A = 10^{-4} particles (Figure 6) where emission from at least two domains is evident. The fact that the blue shifted peaks do not shift with solvent polarity, while the red shifted peaks do, is further support for this multisite scenario. As the D/A is increased further, the more-abundant polar amine sites are predominately labeled, thus dansyl primarily senses this environment. This result is consistent with the observation of only one emission peak that shifts with solvent dipolarity that is seen for the D/A = 0.6 to 10^{-3} particles.

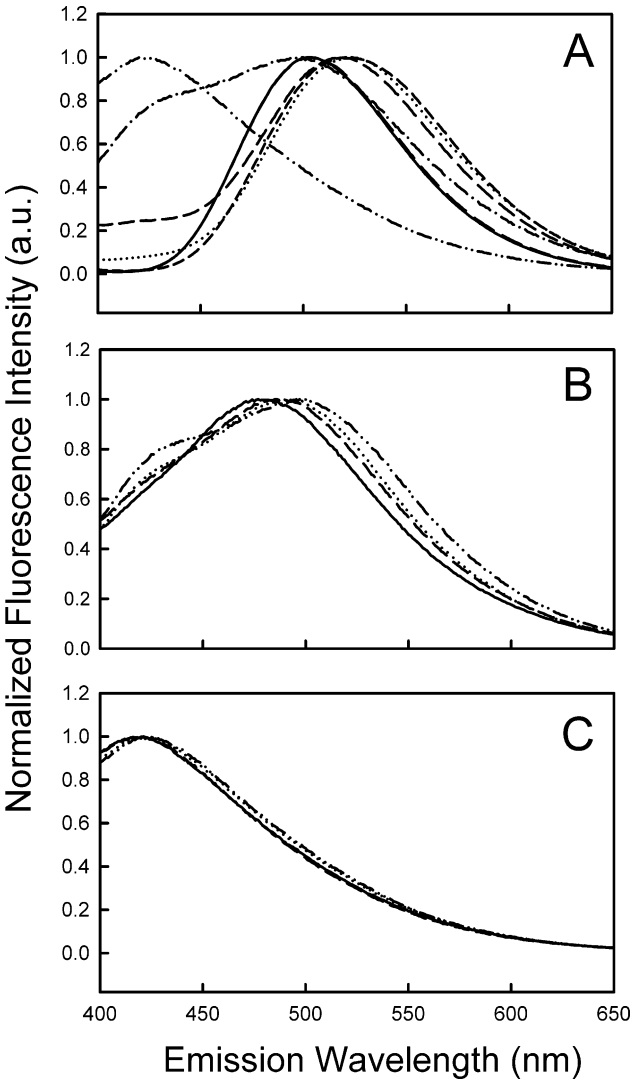

Figure 7. Steady-state emission spectra for silanized D-CPG. (Panel A) In liquid methanol at D/A = 0.6 (—), 0.3 (— — —), 0.1 (— — —), 10^{-2} (- - -), 10^{-3} (· · ·), 10^{-4} (— · —), and 10^{-5} (— ·· —). (Panel B) As a function of solvent at D/A = 10^{-4}. (Panel C) As a function of solvent at D/A = 10^{-5}. The liquids in Panels B and C are hexane (—), ethyl acetate (— — —), 1-butanol (· · ·), and methanol (— · —).

Figure 7 presents the normalized steady-state emission spectra of silanized D-CPG in liquid methanol as a function of D/A (Figure 7A) along with spectra obtained for silanized D-CPG with a D/A of 10^{-4} (Figure 7B) and 10^{-5} (Figure 7C) in various liquid organic solvents. The spectral trends shown in Figure 7A follow the same basic behavior as we saw in unsilanized D-CPG (Figure 6A). The dansyl reporter groups on the D/A = 0.6 to 10^{-3} particles sense a polar environment ($\lambda_{em} \approx 520$ nm). However, a second peak in the dansyl emission spectrum begins to develop for the silanized particles with a D/A of 10^{-2} and it becomes progressively more evident as the D/A decreases to 10^{-4}. The two emission peaks are clearly evident in the other solvents studied (Figure 7B), indicating that it is not peculiar to methanol. [Note: The same arguments that we gave for the unsilanized D-CPG hold here for the silanized D-CPG/hexane results.] A similar emission profile is seen for the unsilanized D-CPG particles with a D/A = 10^{-4} (Figure 6B); however, the intensities of the two emission peaks vary significantly in comparison to

(79) Li, Y. H.; Chan, L.-M.; Tyer, L.; Moody, R. T.; Himel, C. M.; Hercules, D. M. *J. Am. Chem. Soc.* **1975**, *97*, 3118−26.

(80) Wirth, M. J.; Smith, E. A.; Anthony, S. R. *J. Chromatogr., A* **2004**, *1034*, 69−75.

the silanized particles with a D/A = 10^{-4}. Thus, we can conclude that the dansyl groups are simultaneously reporting from at least two distinct microenvironments on the silanized CPG particles too and silanization alters the dansyl cybotactic region, relative to unsilanized D-CPG. That is, the distribution of the dansyl molecules between the solvent inaccessible/restrictive domain (e.g., pore(s)) and the solvent accessible environment(s) is(are) altered for silanized D-CPG when compared to unsilanized D-CPG. At the lowest D/A (10^{-5}), we again see a single emission peak that is blue shifted (maximum at ~422 nm) and whose position is solvent independent (Figure 7C). These results are consistent with the dansyl groups being distributed in hydrophilic, solvent-accessible, and hydrophobic solvent-inaccessible/restrictive domains in silanized D-CPG.

Comparison of the solvent-dependent emission spectra for silanized D-CPG (Figure 7B) and unsilanized D-CPG (Figure 6B) at D/A = 10^{-4} show that the dansyl groups on silanized D-CPG are affected less by solvent in comparison to unsilanized D-CPG. Specifically, the emission maxima from the red spectrum, which corresponds to the dansyl population in the more-accessible site(s), do not shift much with solvent dipolarity in comparison to unsilanized D-CPG at similar D/A values. Furthermore, the intensity ratios of the two emission peaks observed for the silanized D-CPG particles (Figure 7B) do not change too much with solvent dipolarity in comparison to the unsilanized D-CPG particles (Figure 6B). Thus, silanization of the D-CPG particle surface yields a less-heterogeneous cybotactic region for the more-accessible dansyl site(s) in comparison to unsilanized D-CPG.

Conclusions

Solvation of molecules attached to interfaces is much different in comparison to the solvation of "isolated" molecules in solution. Unlike in solution, surface-bound molecules can be surrounded by other molecules, they can be distributed within an ensemble of sites with differing physicochemical properties, and/or they can be distributed in sites that are inaccessible/restrictive to solvent. All of these scenarios are observed for dansylated controlled pore glasses in liquid organic solvents. A simple model (Figure 8) can be used to explain our D/A-dependent observations on silanized and unsilanized D-CPG. Figure 8A summarizes the behavior on unsilanized D-CPG. At the highest D/A (0.6 and 0.3), the surface consists mainly of dansyl clusters/islands where the emitting dansyl molecules are "solvated" by other dansyl groups and liquid solvents do not alter the dansyl cybotactic region significantly. As the D/A decreases (0.1 to 10^{-4}), the average distance between the dansyl groups increases (the relative number of isolated dansyl groups increases), the cybotactic region sensed by the dansyl reporter groups changes, and solvent is able to access/solvate/wet these dansyl residues. However, the extent of solvation is never like that seen for the isolated dansyl molecules in solution. As the D/A is decreased further (10^{-5}), the dansyl groups distribute themselves to an inaccessible/restrictive SiO_2-rich sites within the CPG (e.g., small pores).

Figure 8B summarizes the effects of solvent and D/A on the behavior of silanized D-CPG. At high D/A (0.6 and 0.3), the dansyl groups sense other dansyl molecules and silanization does not alter their cybotactic region significantly. At intermediate D/A (0.1 to 10^{-4}), the majority of free aminopropyl and silanol groups become silanized, thus these dansyl groups sense the newly formed trimethyl

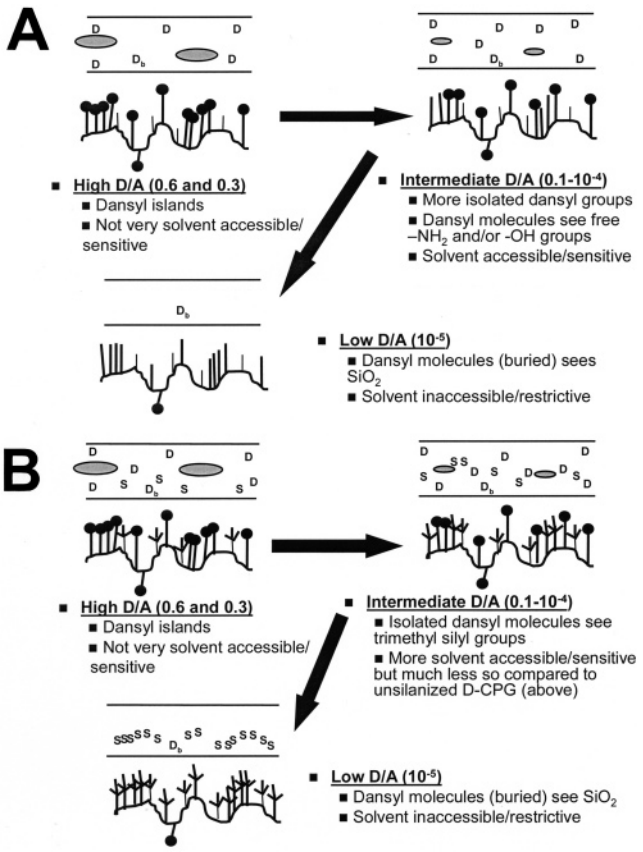

Figure 8. Model describing the effects of D/A, solvent, and silanization on dansylated CPG. (Panel A) Unsilanized D-CPG. (Panel B) Silanized CPG. Legend: Thick lines represent aminopropyl groups. Thin lines denote silanol groups. Black circles represent dansyl molecules. Gray ovals denote islands/ clusters of dansyl molecules. D represents isolated dansyl groups. D_b denotes dansyl groups buried within small pores. S represents trimethyl silyl groups.

silyl groups, providing a more uniformly dipolar surface in comparison to the corresponding unsilanized D-CPG particles. The dansyl reporter groups on the silanized D-CPG are also less sensitive to changes in solvent polarity in comparison to the dansyl groups on the equivalent unsilanized D-CPG particles. This result arises because access to or wetting of the dansyl molecules is controlled by the trimethyl silyl groups. At the lowest D/A value (10^{-5}), the dansyl groups again appear insensitive to silanization because these dansyl moleules are located in an inaccessible/restrictive domain within the CPG (e.g., small pores).

These results contribute to an improved molecular-level understanding of the surface of aminopropyl-modified silica as a function of surface loading and surface modification (e.g., end capping). This work has several implications when considering the common use of aminopropylated CPG as a solid support for the *covalent attachment* of reagents in the separation sciences, solid-phase catalysis, and chemical sensing. For example, this work lends further credence to the idea of low concentrations of "strong sites" causing chromatographic band tailing[80] and cluster/island formation.[51]

Acknowledgment. This work was generously supported by the US Department of Energy.

LA0490184